(2)

Naval Research Laboratory

Washington, DC 20375-5000

NRL Memorandum Report 6770

AD-A232 649

Density Channel Tracking Studies on Pulserad

D. P. MURPHY, R. E. PECHACEK, D. P. TAGGART,* R. A. MEGER

Charged Particle Physics Branch
Plasma Physics Division

* *Los Alamos National Laboratory*
Los Alamos, NM 87545

March 2, 1991

Approved for public release; distribution unlimited.

REPORT DOCUMENTATION PAGE

Form Approved
OMB No 0704-0188

1. AGENCY USE ONLY (Leave blank)	2. REPORT DATE	3. REPORT TYPE AND DATES COVERED
	1991 March 2	

4. TITLE AND SUBTITLE

Density Channel Tracking Studies on Pulserad

5. FUNDING NUMBERS

47-2699-0-0 PE 62707E
47-0922-0-0 PE 0601153N

6. AUTHOR(S)

D. P. Murphy, R. E. Pechacek, D. P. Taggart,* and R. A. Meger

7. PERFORMING ORGANIZATION NAME(S) AND ADDRESS(ES)

Naval Research Laboratory
4555 Overlook Ave., S.W.
Washington, DC 20375-5000

8. PERFORMING ORGANIZATION REPORT NUMBER

NRL Memorandum Report 6770

9. SPONSORING/MONITORING AGENCY NAME(S) AND ADDRESS(ES)

ONR
Arlington, VA 22217-5000
NSWC
10901 New Hampshire Ave., Silver Spring, MD 10903-5000

10. SPONSORING/MONITORING AGENCY REPORT NUMBER

11. SUPPLEMENTARY NOTES

*Los Alamos National Laboratory, Los Alamos, NM 87545

12a. DISTRIBUTION/AVAILABILITY STATEMENT

Approved for public release; distribution unlimited.

12b. DISTRIBUTION CODE

13. ABSTRACT *(Maximum 200 words)*

High current charged particle beams can be guided by reduced density channels. This tracking occurs when the distribution of plasma currents in the density channel causes a net attractive force to be exerted on the electron beam. A relativistic electron beam (REB) injected parallel to a spatially offset reduced density channel is pulled toward the channel. The force exerted on the beam is predicted to increase as the beam current increases and as the offset between the beam and the channel increases out to offsets equal to the beam radius. An experiment with a 1-MV, 10 kA beam was performed which demonstrates this effect.

14. SUBJECT TERMS

Electron beam   Density channel
Tracking

15. NUMBER OF PAGES

35

16. PRICE CODE

17. SECURITY CLASSIFICATION OF REPORT	18. SECURITY CLASSIFICATION OF THIS PAGE	19. SECURITY CLASSIFICATION OF ABSTRACT	20. LIMITATION OF ABSTRACT
UNCLASSIFIED	UNCLASSIFIED	UNCLASSIFIED	SAR

NSN 7540-01-280-5500

Standard Form 298 (Rev 2-89)
Prescribed by ANSI Std Z39-18

CONTENTS

DENSITY CHANNEL TRACKING STUDIES ON PULSERAD

I. INTRODUCTION

The existence of a mechanism which would allow electron beams to track preformed density channels is a key element for long range propagation of Charged Particle Beams (CPBs). Most endoatmospheric CPB propagation schemes envision multiple beam pulses boring a hole in the atmosphere as the beam packet propagates. The first or lead pulse of the packet propagates in a uniform density gas background. As it propagates it deposits its energy in the gas, heating it and producing a reduced-density channel. If succeeding pulses follow the density channel produced by the earlier pulses they would lose less energy in the lower density gas than they would outside it. Eventually they would emerge from the end of the preformed channel, become lead pulses themselves and extend the channel. In this way the range of the CPB propagation can be extended beyond the uniform density limit.

An experiment using a single pulse accelerator and preformed reduced-density channels was carried out to test the basic physics. The goal of the research was to experimentally test a tracking mechanism discovered by Welch in simulations of electron beams propagating through initially un-ionized air.[1] A summary of these numerical studies and the results of a recent tracking experiment performed by Bieniosek at McDonnell Douglas Research Labs using shallow density channels is given in reference #1. The theory suggests that a positive tracking force exists between a density channel and an electron beam arising from asymmetric plasma current flow in the channel induced by the beam. The strength of the tracking force is predicted to increase with the beam current and is a function of the channel depth and the beam offset relative to the channel axis. The 1MeV beams in this experiment were produced by the 1-MV Pulserad 310 electron beam generator[2], and the reduced density channels were produced by the technique of Laser Guided Electric Discharges (LGED).[3] The electron beam pulses were about 35ns long and had nominal peak beam currents of 9-12kA in the first experimental run (summer 1987) and currents of 5-10kA in the second experimental run (summer 1988) depending on the anode-cathode (AK) gap selected in the Pulserad diode. The channels were offset relative to the beam axis by ±1cm in the first run and by 0cm, ±1.4cm or ±2.6cm in the second run. The conducting chamber wall radius was 45cm in both experiments in order to minimize wall centering effects.

II. DENSITY CHANNEL TRACKING THEORY

The basis of the density tracking effect can be understood from an analytic theory developed by R.F. Fernsler.[4] In this model a cylindrical reduced-density channel is

Manuscript approved December 19, 1990.

surrounded by a uniform, higher density background gas distribution. The beam is initially displaced off the channel axis by a distance y_c. The theory is based on three key elements:

- Ionization of the background gas is dominated by direct beam ionization. This yields an ionization fraction, n_e/n_g (n_e=electron density, n_g=local gas density), on the beam timescale that is independent of the background density and is symmetric about the beam. The weak plasma fully neutralizes the beam's space charge.
- The plasma electrons produced by the beam are accelerated and heated by the nearly uniform axial inductive electric field, E, produced by dI_{eff}/dt where I_{eff} is the effective current (beam minus plasma current) within the radius of the beam. The plasma electron temperature in this weakly ionized gas depends on the reduced field strength E/n_g. Therefore the electron temperature in the lower density channel will be higher than that in the surrounding region.
- The return current driven by the inductive electric field depends on the electron-neutral collision frequency in the background plasma. For electron temperatures up to several electron volts the collision frequency increases with the plasma electron temperature for most atmospheric gases. Thus the resistivity, which is proportional to the collision frequency, will be higher in the lower density central region than in the higher density regions near the edge of the channel. The return current driven by the inductive electric field will therefore flow preferentially in the lower resistivity regions near the edges of the channel. When the beam and the channel are offset the plasma return current distribution will be asymmetric about the channel axis. The dipole component of this plasma current interacting with the beam current provides the centering force on the beam which causes the beam to track the channel.

Figure 1 shows the predictions of the non-linear, analytic force equation, as discussed in Appendix I. For a beam and channel similar to that used in the experiment described below, the tracking force as a function of the offset between the channel and beam is predicted to increase from zero to a peak near the channel radius. At larger offsets the force decreases. The tracking length, which is the propagation distance necessary for the beam to cross the channel axis, is independent of the offset, unless the offset is comparable to or larger than the beam or channel radii. The tracking force increases linearly with the plasma return current and weakly with the channel gas density. Figure 2 shows a plot of the tracking length versus relative channel gas density. The tracking length monotonically increases as the channel depth decreases. The beam must be stable over the tracking length in order to see the effect clearly. Tracking lengths for the pulserad experiments range from under 40cm to over 1m, depending on the beam and channel parameters.

III. EXPERIMENTAL CONSIDERATIONS

Several effects not treated in the theory must be taken into account for a viable experiment is to be performed. The beam profile is degraded by scattering off the background gas, increasing the beam radius. The beam is also subject to the hose instability which can drive the beam out of its intended trajectory. Scale lengths for these effects can be calculated and compared with the tracking length.

A measure of the effect of scattering off the background gas is the Nordsieck length, L_n, which measures the propagation length over which the beam radius e-folds due to scattering. A rough expression for the Nordsieck length is:

$$L_n = 6.1 \frac{(\gamma I_{eff})^{0.93}}{n/n_o} \; cm \tag{1}$$

where I_{eff} is the net current within the radius of the beam, i.e.,

$I_{eff} = 2\int_0^\infty 2\pi r \frac{j_b}{I_b} dr \int_0^r 2\pi r' \left[j_b + \sigma E_z\right] dr'$ and n/n_o is the relative gas density. This expression for the Nordsieck length is a fit to numerical simulations by Hughes and Godfrey.[5] Figure 3a shows the Nordsieck length as a function of relative channel density and beam current. The beam is assumed to remain inside the channel which significantly increases L_n for a low density channel. The tracking length for even a low current beam and 50% deep channel is less than or equal to the Nordsieck length. Thus, Nordsieck expansion should not dominate the tracking length measurement.

The hose instability is more difficult to overcome experimentally. It can be strong enough to drive the beam off its initial trajectory and overcome a positive tracking force. Once the beam leaves the channel the tracking force drops quickly (see fig.1). Even if the beam is not driven out of the channel the tracking effect can be masked by moderate hose oscillations. Ideally, a completely hose stable beam should be used, but for a demonstration of the tracking effect a beam which is stable for over a tracking length is sufficient. A scale length for the growth of the hose instability is the betatron wavelength given roughly by:

$$L_b = 2\pi r_b \left[\frac{I_A}{I_{eff}}\right]^{1/2} \tag{2}$$

where I_A is the Alfvén current (17$\beta\gamma$ kA), $\beta = v_z/c$ is the normalized electron velocity and $\gamma = (1-\beta^2)^{-1/2}$ is the relativistic scaling factor. For Pulserad γ=3. Figure 3b shows the

calculated betatron wavelength as a function of beam radius. For the Pulserad beam $L_b \approx$ 20-40cm.

A third phenomena which can negate a positive tracking force is electron avalanche in the low density channel. When the inductive electric field produced by the rising current exceeds the avalanche ionization threshold level ($\approx$ 50kV/cm-atmosphere for air), the collisionally produced plasma electrons gain enough energy from the field to produce avalanche ionization. This threshold is lowest on the reduced density channel axis. If the channel avalanches, the additional plasma return current will drive the beam out of the channel. A simplified expression for the inductive electric field near the head of the beam is:

$$E_z = \frac{I_{eff}}{T_r} \ln\left(\frac{r_w}{r_b}\right) kV/cm, \tag{3}$$

where for these experiments T_r(ns) $\approx$ 10ns is the risetime of I_{eff}(kA) and r_w is the wall radius, ($r_w/r_b \approx$25). Figure 3c shows a family of curves of the axial field normalized to the avalanche threshold. At high currents and low channel density the threshold is exceeded which should result in repulsion of the beam from the channel.

A similar effect could result due to the presence of free electrons in the channel prior to beam injection. The LGED method used to produce the rarefied channels leaves the channel ionized with a non-zero conductivity for a short time after production. If the DC conductivity level is more than $\approx 5\text{x}10^9$ sec^{-1}at beam injection, there are enough free electrons in the channel for the beam to drive sufficient on-axis return current to expel the beam from the channel.[4] The LGED channel is considerably above this threshold value when first created. The channel cools by adiabatic expansion during the first few hundred microseconds and by turbulent convective mixing of background gas into the hot channel on a several millisecond timescale. The colder, higher-density gas near the edges moves toward the channel axis as highly asymmetric three-dimensional flutes with a scale length on the order of the channel radius. Depending on the total energy dumped into the channel, 2ms or more must elapse before beam injection to prevent the beam from being driven out of the channel.

Lastly, higher-order chemistry processes not considered in the theory can produce detracking late in the beam pulse. These processes include electron-ion recombination, electron attachment, and Spitzer collisions. This detracking is usually offset, however, by longitudinal magnetic coupling. Coupling causes the beam body to follow the head and dominates once the plasma conductivity is large.[4] Thus, if the head tracks the channel, the body and tail should also. The higher-order chemistry processes do, however, reduce

the peak tracking force, thereby producing tracking distances longer than predicted by the simple analytic theory. Slinker[7] and Keeley[8] have conducted detailed numerical studies of the effects of higher-order chemistry, including water vapor, on tracking.

IV. EXPERIMENTAL TECHNIQUE

Figure 4 shows schematic views of the interaction between the REB and a displaced reduced-density channel in the experimental setups used for the two data runs. The chamber was ≈ 90cm inner diameter by 2.5m long and made of lucite lined with copper screen to facilitate optical photography during the experiment. The electron beam from Pulserad was injected into the experimental chamber, on axis, through a beam current monitor. Baseline beam propagation data was obtained by injecting the beam into the chamber with no channel present. In the first experimental run a 9-12kA beam was injected through a 3.0mil titanium (Ti) anode foil into ±1cm offset channels. The net current centroid was monitored with a single set of four magnetic probes mounted on the chamber wall 40cm downstream from the injection point. For the second experimental run beam currents were decreased to 5-10kA at injection and the beam radius was enlarged to about 2.1cm by passing it through an additonal 1.5mil Ti foil. The reduced current and larger radius combined to increase the betatron wavelength (Eq. 2) which improved the beam stability. The net current centroid position was measured by three sets of magnetic probes 20cm, 60cm and 110cm downstream of the injection point. The rarefied channel was offset by ±1.4cm and by ±2.6cm from the chamber axis, or placed directly along the chamber axis. To monitor for systematic errors in the beam injection, measurements were taken in groups of four successive shots: no channel present, channel displaced up, channel displaced down, channel centered on chamber axis. Figure 5 shows a typical beam current pulse measured at injection and the net current 20cm downstream for a no-channel shot. Figure 6 shows the tracking geometry as viewed along the propagation axis for an offset density channel and an electron beam passing along the edge of the channel.

V. CHANNEL PARAMETERS

Extensive measurements were made on LGED channels. Schlieren photography indicated that the channel edge radius increased from below 3cm to about 4cm in the time between 2ms and 5ms after initiation. Turbulent mixing with the surrounding gas appears to be the primary mechanism for decay of the channels. This is characteristic of using an aerosol and a laser to designate the initial breakdown channel in the LGED process. The turbulence produces a region on the sides of the channel with a mixture of high and low density gas. The conductivity generated by the beam passing through this turbulent region should be a mixture of the high and low density conductivities in series. A beam produced channel would not suffer from as strong turbulent mixing. The channel depth infered by Stalder et

al.[6] from early time conductivity measurements and from optical interferometry is ≤ 1/10 atmosphere. The depth of the channel and the diameter are dependent on the bank energy deposited in the LGED process.

VI. CHANNEL TRACKING EXPERIMENTAL RESULTS

VIa.--(First run; Summer 1987)The 9-12kA Pulserad beam used for this run was subject to strong hose instability. On many of the shots the beam diverted toward the wall after propagating to about Z=60cm. The magnetic pickup loops, mounted on the wall at Z=40cm, r_W=45cm, necessarily averaged over the beam motion for some distance along the Z-axis. While it was possible to determine which direction the beam moved if it hosed, the magnitude of the motion was an average. With this caveat in mind, figure 7 presents the net current centroid measurements for this run. The delay time between channel creation and beam injection was 500-3500μs. The shot data has been normalized to the direction of the channel offset such that motion towards the channel is positive and motion away from the channel is negative. The shots with no channel present are the last set shown in Fig. 7 and are designated by the "NO-CH" label. At each delay time the data is subdivided to show the motion in the beam head (10ns), beam body (20ns) and the beam tail (30ns). The data shows the beam head pulled in first, the the body and tail follow, as expected. The error bars represent one standard deviation about the average of the shots taken at that particular delay time. For time delays ≤ 2ms the beam was ejected from the channel, probably due to thermal ionization in the still hot channel. After a delay of 2.5ms or more, the beam moved toward the channel indicating that the channel had cooled enough to permit the tracking force to come to the fore. Measurements of the bulk channel DC conductivity indicated that it dropped below the theoretically predicted threshold of $5x10^9$ sec^{-1} for avalanche ionization at that time. Since the no-channel shots were not grossly unstable until well past the probe position, there is evidence that the channel was triggering increased hose instability. On several shots the beam seemed to move completely through the channel on its way to the wall, consistent with numerical simulations by Taylor et al.[9]. Theoretical predictions for the tracking length of a >10kA beam with a beam radius of about 1.5cm and a 1cm offset channel yield lengths less than 100cm. The data from this high curent first run hint at a short tracking length but the hose motion of the beam made it impossible to extrapolate a valid number from the data. Simulations by Taylor et al. agree with the experimental results.[9]

VIb.--(Second run; Summer 1988)The 5-10kA Pulserad beam used for this run was much more stable because the beam current was reduced and the beam radius increased from the first run. These changes also increase the tracking distance Z_t, however, as was observed. Three sets of magnetic probes were mounted on the wall (r_W=45cm) at Z=20cm,

60cm and 110cm in order to more accurately track the trajectory of the beam. It was found that for injected currents ≤ 9kA the beam was hose stable for the entire length of the propagation range. Figure 8 presents for the no-channel shots the average beam trajectory at three times during the pulse. The error bars represent one standard deviation about the average. Since the channel offsets were ±1.4cm and ±2.6cm the beam motion was acceptably small. As with the first run the beam was ejected from a hot channel (delay time ≤2ms). Figure 9 illustrates this phenomenon with the average trajectory for beams injected into the chamber with a 2.6cm offset channel and short delay times. The channel size and position are represented by the shaded region in the figure.

For delay times ≥ 3ms (and peak beam currents still ≤ 9kA) the trajectories for shots with the channel along the chamber axis were little different than those shots without a channel present. The average over all the shots in the set, shown in figure 10, indicates that the beam trajectories track exactly on the channel axis and the spread of the trajectories was not much larger than that of the no channel shots. The small difference between these two data sets indicates that the channel did not induce more than a small increase in the hose instabliity of the beam.

The next two figures show the beam motion in the presence of offset channels, again for delay times ≥ 3ms and injected currents ≤ 9kA. Figure 11 shows the average trajectory for the ±1.4cm offset channel shots. There was a small movement of the beam of about 1cm toward the channel, principally at the peak of the current pulse where the tracking force is strongest, but the scatter in the data made it impossible to extrapolate a tracking length from this data set. The analytic theory predicts the tracking force should increase as the offset between the beam and channel increases, out to the channel edge, but the tracking length itself increases monotonically as the offset increases. This prediction was supported by the 2.6cm offset channel data presented in figure 12. The average beam offset at peak current was more than 2cm towards the channel center, with acceptably small scatter in the data, at the Z=110cm probe position. Extrapolating the average trajectory at peak current through the 20cm, 60cm and 110cm data points to the channel axis yields a tracking length of $Z_t \approx 160$cm. This value for Z_t is consistent with current numerical simulations. The channels are about $1/10$ *th* density at center shortly after being created but they fill in asymmetrically due to turbulence as the channel cools. The profiles are somewhat ragged due to this convective mixing of cold outside gas into the hot channel which makes for a higher average density and an increase in the tracking length due to a reduction in the attractive force. From figure 1 a reasonable match to the present experiment is the calculation of the interaction between a 5kA beam with a Bennett radius of 2.3cm and a 2.6cm offset channel with a half density radius of 2.5cm and a channel density about 0.5 that of ambient which yields a calculated tracking length of 150cm. This is fairly good

agreement between theory and experiment considering the difficulty in determining even an approximate profile of the density channel for use in the calculations.

VII. DISCUSSION AND SUMMARY

Both experiments demonstrated clearly the existence of a density tracking force, as well as a detracking force at high levels of cnannel preionization. Furthermore, the transition from detracking to tracking occurred at the expected channel overheat condition.[4] Although the tracking length and overall beam motion agreed qualitatively with theory and numerical simulations,[9] precise quantitative comparison was hampered by uncertainties in the experimental parameters and by complications from the hose instability.

The largest uncertainties are the channel density profile and the beam radius. The on-axis channel density was $\approx$ 0.1atm shortly after being created, but then gradually rose as the channel cooled and filled in asymmetrically due to convective mixing with surrounding air. Although the complicated spatial structure of the channel makes its density profile difficult to characterize and diagnose, average values can be inferred using particle conservation and measured values of the (ragged) channel edge radius. The beam radius is similarly not well known but presumably was considerably larger in the second set of experiments, as indicated by the longer tracking distances and more stable beam behavior.

Hose instability precluded demonstration of improved beam propagation in the reduced-density channels. We hope to avoid this problem in future experiments using the SuperIBEX beam by conditioning the beam prior to propagation. Improved diagnostics will also be employed to provide better comparison with theory.

ACKNOWLEDGEMENTS

We wish to thank E. Laikin, S. Hauver and W. Dolinger for technical assistance in performing these experiments and we thank M. Nash and A. Mital for assistance with the data handling and reduction. Special acknowledgement goes to Dr. M. Raleigh for his help in designing the experiment and for many fruitful discussions which guided the experimental procedure. We also thank Drs. R. Hubbard, R. Taylor and S. Slinker for their theoretical and numerical modeling of this experiment. This work was performed at the Naval Research Laboratory with funding provided by the Defense Advanced Research Projects Agency under ARPA Order 4395, Ammendment No. 86 and monitored by the Naval Surface Warfare Center.

REFERENCES

1. D.R. Welch, F.M. Bieniosek and B.B. Godfrey, Phys. Rev. Lett., 65, 3128 (1990).

2. D.P. Murphy, et. al., 9th Int. Symp. on Eng. Prob. in Fusion Res. (Chicago, 1981) IEEE 81CH1715-2, 1548.

3. J.R. Greig, et. al., Proc. 7th Int. Conf. on Gas Discharges, (London, 1982) and D.P. Murphy, et. al., NRL Memo Report 5688, Feb 1986.

4. R.F. Fernsler, S.P. Slinker and R.F. Hubbard, "Theory of Electron Beam Tracking in Reduced-Density Channels", submitted to Phys. Fluids.

5. T.P. Hughes and B.B. Godfrey, Phys. Fluids, 27, 1531 (1984).

6. K.R. Stalder, M.S. Williams, D.J. Eckstrom, Private Communication.

7. S.P. Slinker, A.W. Ali and R.D. Taylor, J. Appl. Phys., 67, 679 (1990).

8. D.A. Keeley, private communication.

9. R.D. Taylor, R.F. Fernsler, F.F. Hubbard and S.P.Slinker, "Analysis of Channel Tracking in SuperIBEX and Pulserad", NRL Memo Report 6675, Aug. 1990,

APPENDIX I

The non-linear form of the tracking force equation[4] can be evaluated under certain conditions. Assume the total electric field rapidly approaches the axial monopole field E_{zo} and the mobility is a function of the reduced electric field, $\tilde{\mu} = \sigma/n_e = \tilde{\mu}(E/n_g)$. The angular part of the force equation integral evolves to

$$\int_0^{2\pi} d\Theta \cos\Theta\, \tilde{\mu}\, E_z \;\rightarrow\; E_{zo}\int_0^{2\pi} d\Theta \cos\Theta\, \tilde{\mu} \;=\; -E_{zo}\int_0^{2\pi} d\Theta \sin\Theta \frac{d\tilde{\mu}}{d\Theta}$$

$$= -E_{zo}\int_0^{2\pi} d\Theta \sin\Theta\, q\,\tilde{\mu}_o \frac{\partial \ln(n_g)}{\partial\Theta} \; . \quad (A1)$$

Here the form of the mobility is assumed to be

$$\tilde{\mu}(E/n_g) = \tilde{\mu}_o\left[1 - q\ln\left(\frac{E/n_g}{x_o}\right)\right] \qquad (A2)$$

which is fit to published values of the mobility of air using q=0.2 and x_o=100 Townsends. The calculation is closed by assuming a channel density profile given by

$$n_g(r') = n_\infty\left[\frac{(r'/a_c)^2 + \delta}{(r'/a_c)^2 + 1}\right]^p \qquad (A3)$$

$$\text{where}\begin{cases} n_\infty = \textit{ambient gas density} \\ (r')^2 = r^2 + y_c^2 - 2\, r y_c \cos\theta \\ y_c = \textit{channel offset} \\ a_c = \textit{channel radius} \\ \delta^p = \textit{channel depth} \\ p \in [0 < p \leq 10\,] \\ \delta < 1 \end{cases}$$

Since an exact channel profile could not be determined a range of values for a_c, p and δ were chosen for a parameter study.

The partial derivative in (A1) can be expanded as follows:

$$\frac{\partial\, \ln(n_g)}{\partial\Theta} = \frac{2py_c\, r\sin\Theta}{r^2 + y_c^2 + \delta a_c^2 - 2y_c\, r\cos\Theta} - \frac{2py_c\, r\sin\Theta}{r^2 + y_c^2 + a_c^2 - 2y_c\, r\cos\Theta} \; . \qquad (A4)$$

The tracking force equation, $F_t = qE$, can be integrated and yields an asymptotic tracking force given by:

$$F_t = -\frac{2e^2\pi}{y_c\, c}\, pq \int_0^\infty \frac{dr}{r}\, I_b \left[\frac{n_e}{n_g}\right] E_{zo} \left\{ \begin{array}{c} a_c^2\,(1-\delta) \\ +\left[r^4 + 2r^2\,(\delta a_c^2 - y_c^2) + (y_c^2 + a_c^2)\right]^{1/2} \\ -\left[r^4 + 2r^2(a_c^2 - y_c^2) + (y_c^2 + a_c^2)^2\right]^{1/2} \end{array} \right\} \tag{A5}$$

where the plasma current is $I_p = I_b - I_{eff} \approx 0.3\ I_b$ at the peak of the Pulserad beam pulse. Direct production causes $\left[\frac{n_e}{n_g}\right]$ to be self-similar with J_b. Then assuming a Bennett beam with radius a_b one can integrate (A5) to obtain:

$$F_t = \frac{qp}{2k}\left(\frac{eI_p}{y_c c}\right)\left[g_1(1) - g_1(\delta)\right] \quad \textit{where} \tag{A6}$$

$$g_1(\delta) = \frac{(2a_b\, a_c\, y_c)^2}{d^3}\,\delta\,\ln(\alpha) + \frac{y_c^4 - (a_b^2 - \delta a_c^2)^2}{d^2} \tag{A7}$$

$$d\,(\delta) = \left[\,(y_c^2 + \delta a_c^2)^2 + 2a_b^2\,(y_c^2 - \delta a_c^2) + a_b^4\right]^{1/2} \tag{A8}$$

$$\alpha\,(\delta) = \frac{(d + \delta a_c^2 - y_c^2 - a_b^2)\,a_b^2}{d\,(y_c^2 + \delta a_c^2) + (y_c^2 + \delta a_c^2)^2 + a_b^2(y_c^2 - \delta a_c^2)} \tag{A9}$$

$$k\,(\delta) = 1 - q\ln\left(\frac{E/n_\infty}{x_o}\right) + \frac{pq}{2}\left[\,\ln(\delta) + g_2(1) - g_2(\delta)\right] \tag{A10}$$

$$g_2(\delta) = \frac{y_c^2 + \delta a_c^2 + a_b^2}{d}\,\ln\,(\alpha)\ . \tag{A11}$$

The tracking distance, Z_t, which represents the propagation length necessary for a beam to be pulled to the channel axis is:

$$Z_t \approx \frac{c\,\tau}{4} = \frac{\pi}{2}\left(\frac{\gamma\, m\, c^2\, y_c}{F_t}\right)^{1/2} \tag{A12}$$

which is independent of y_c only for $y_c \to 0$.

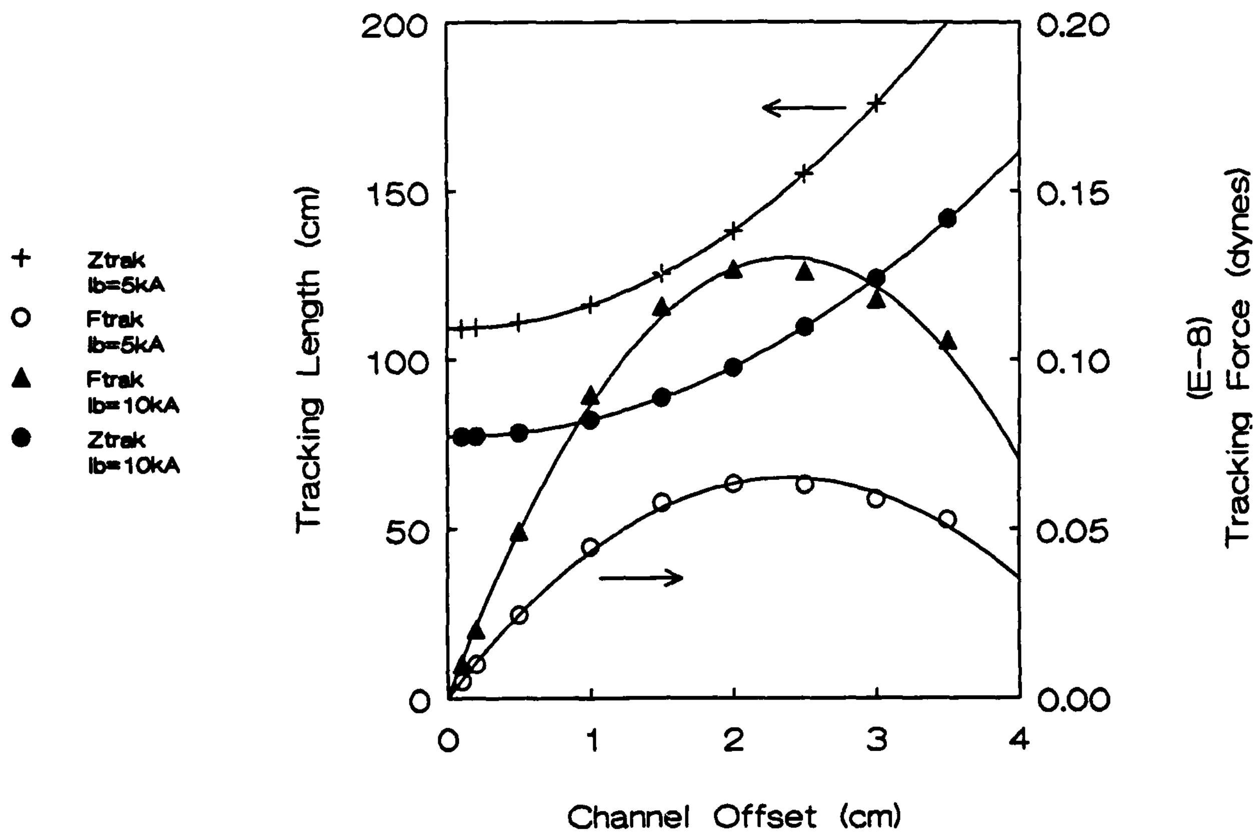

Figure 1. Pulserad Simulation of the tracking force and the tracking length for Relative Channel Density=0.5, Channel Radius=2.5cm, Beam Radius=2.3cm and γ=3.

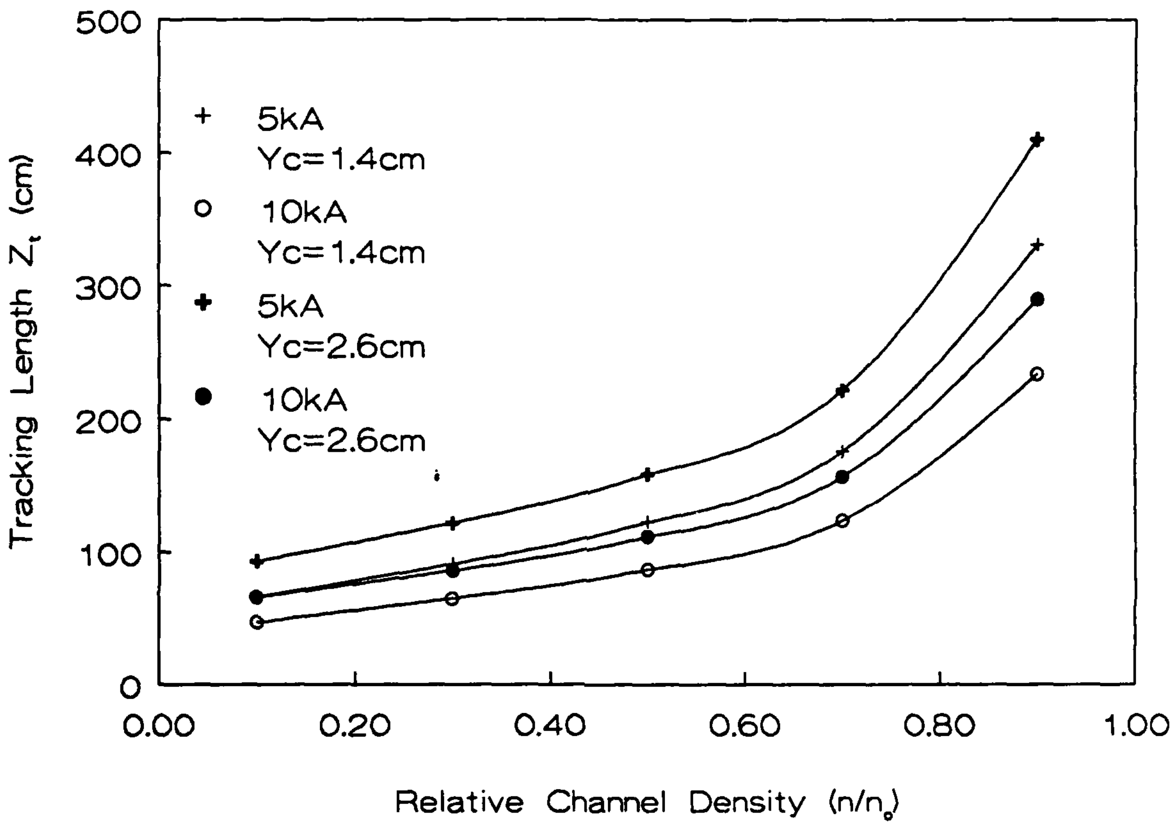

Figure 2. Approximate tracking length using nonlinear theory for the Pulserad beam with r_b=2.3cm and r_c=2.5cm

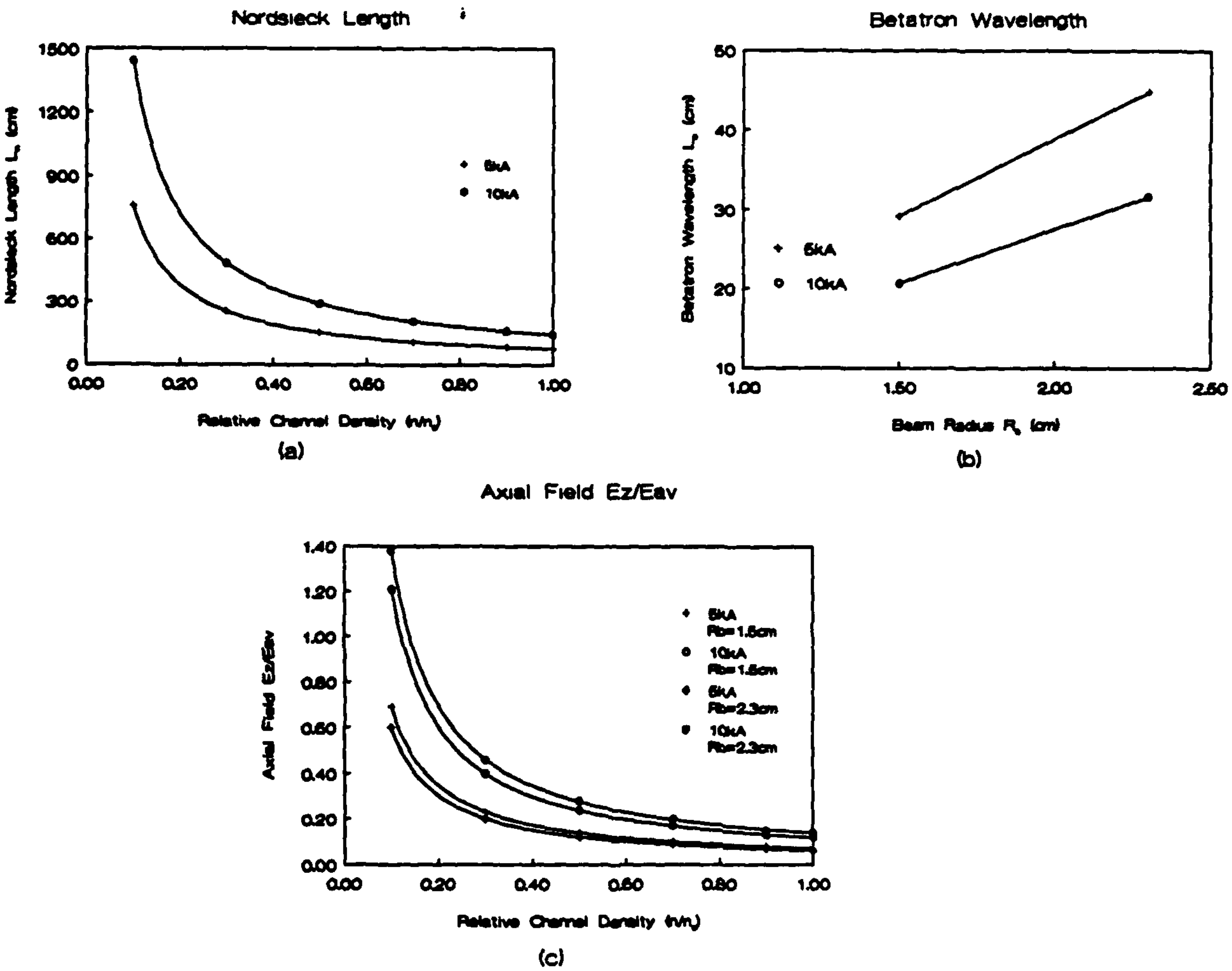

Figure 3. Calculated Pulserad Beam Propagation and Stability Parameters.

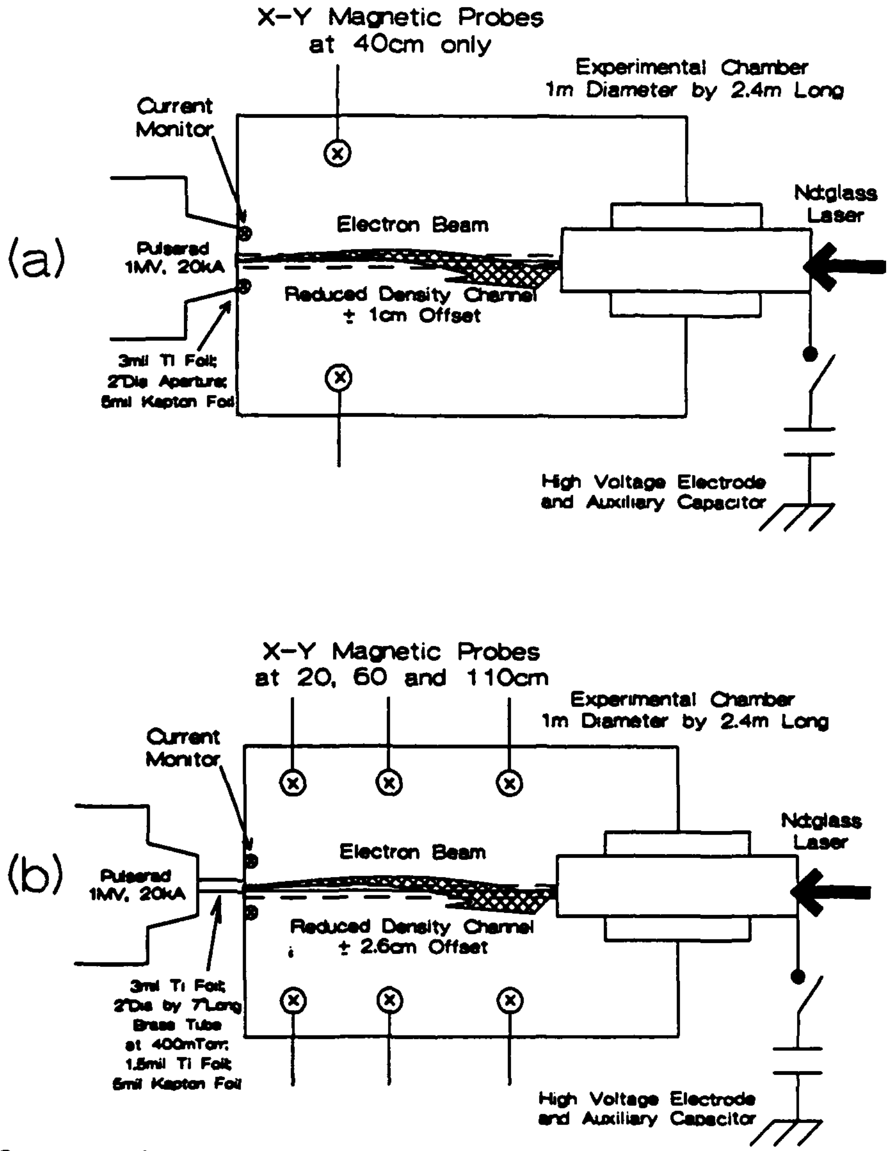

Figure 4. Schematic diagram of the two propagation chambers used in the two experimental runs.

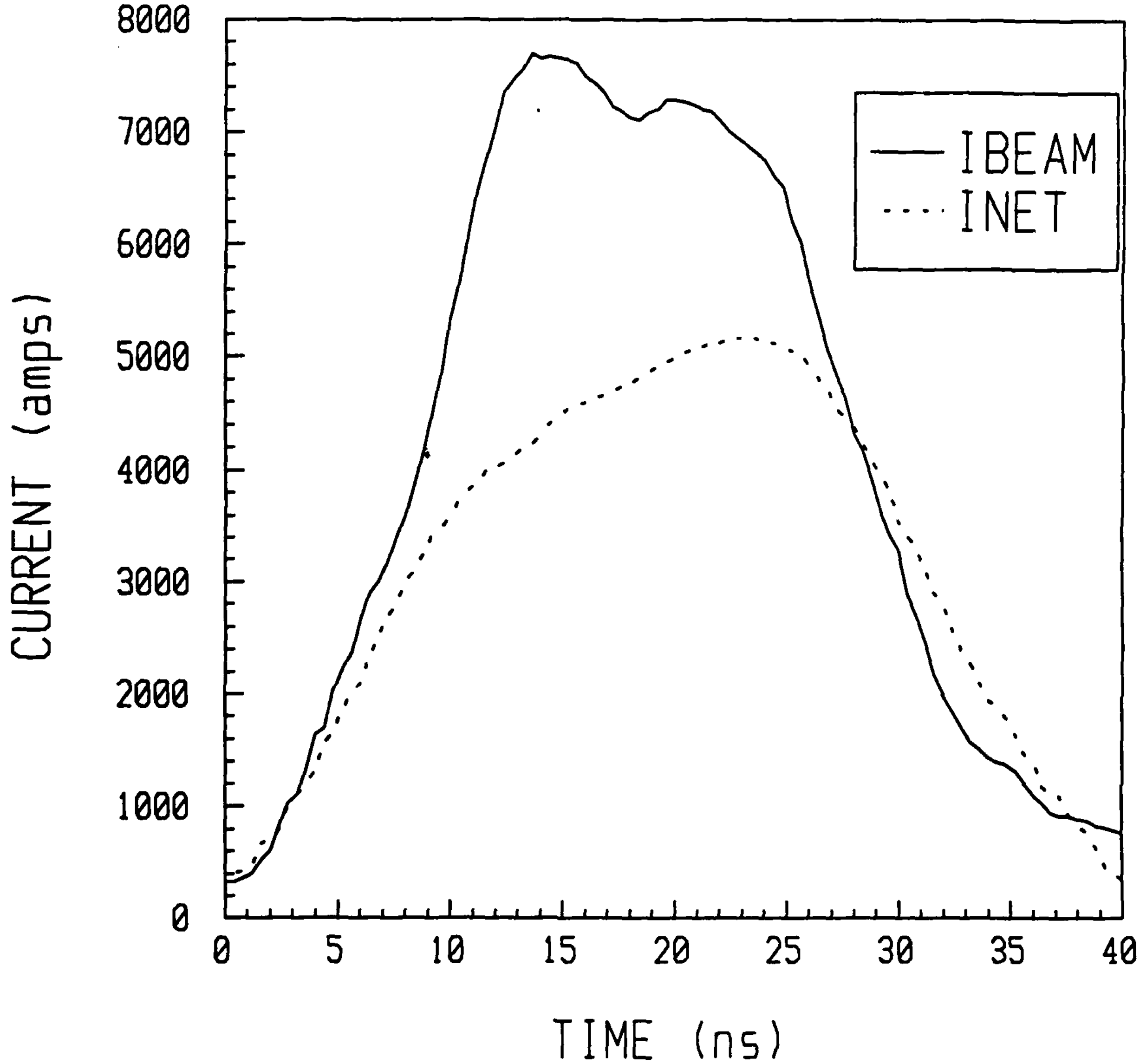

Figure 5. Beam current measured at injection and net current measured 20cm downstream with no channel present.

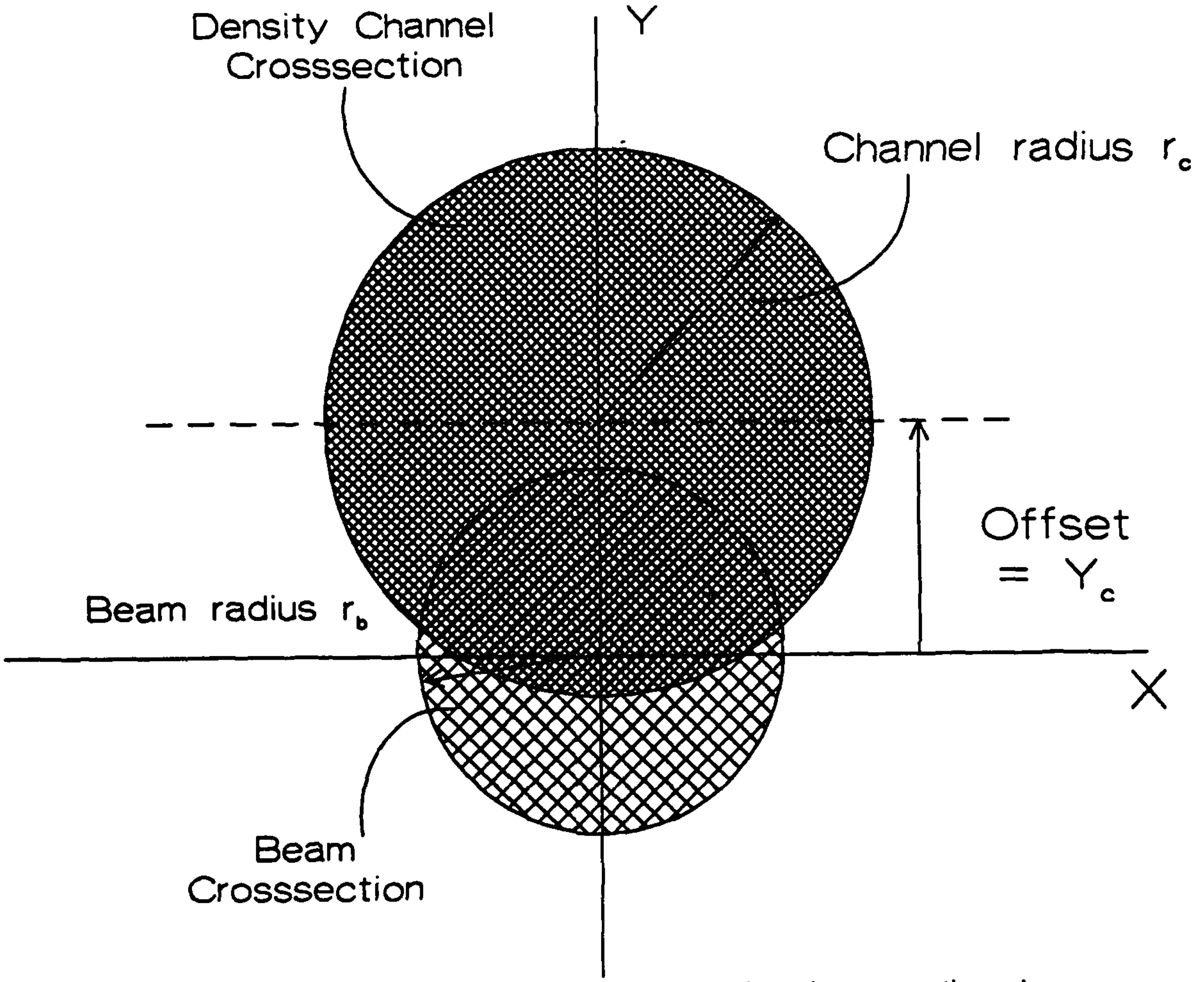

Figure 6. Pulserad tracking geometry as viewed along the propagation axis.

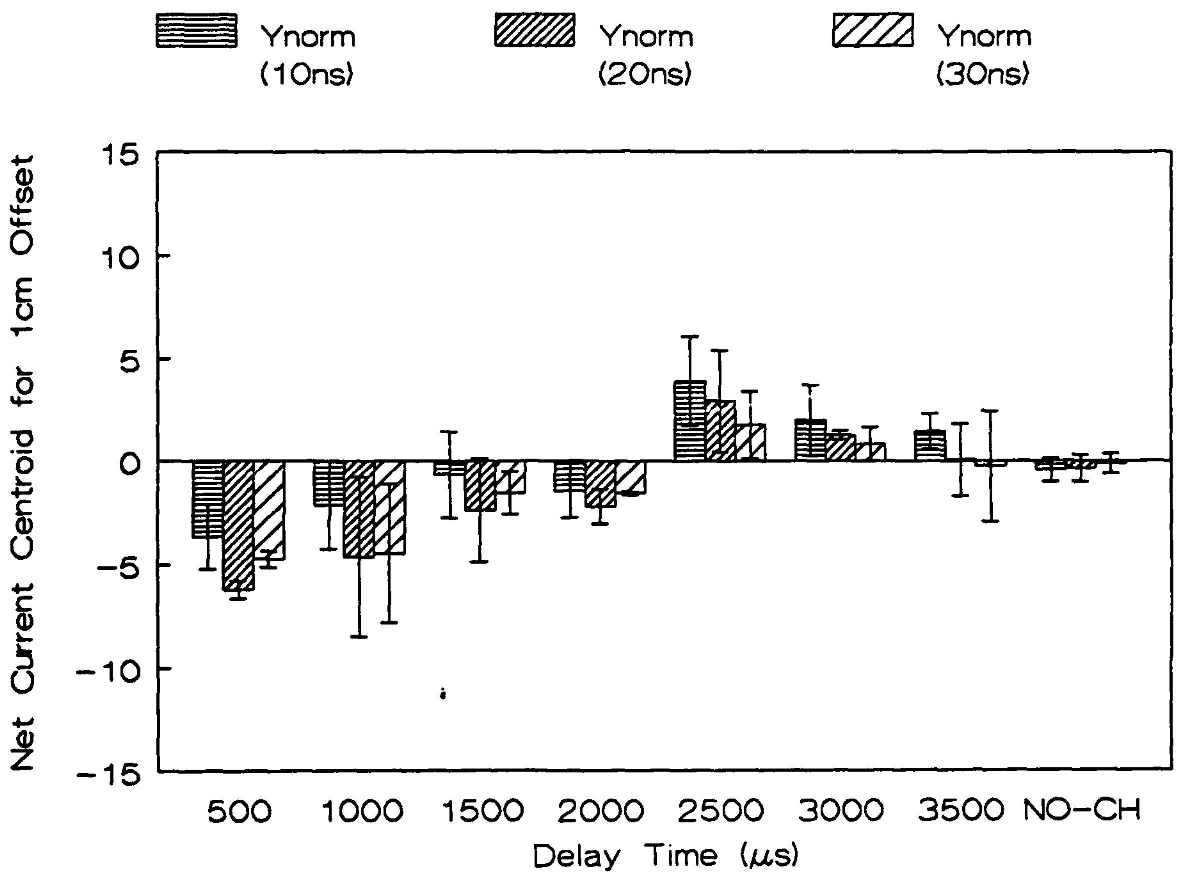

Figure 7. '87 Channel Tracking Experiment results for net current centroid motion versus delay time after channel creation.

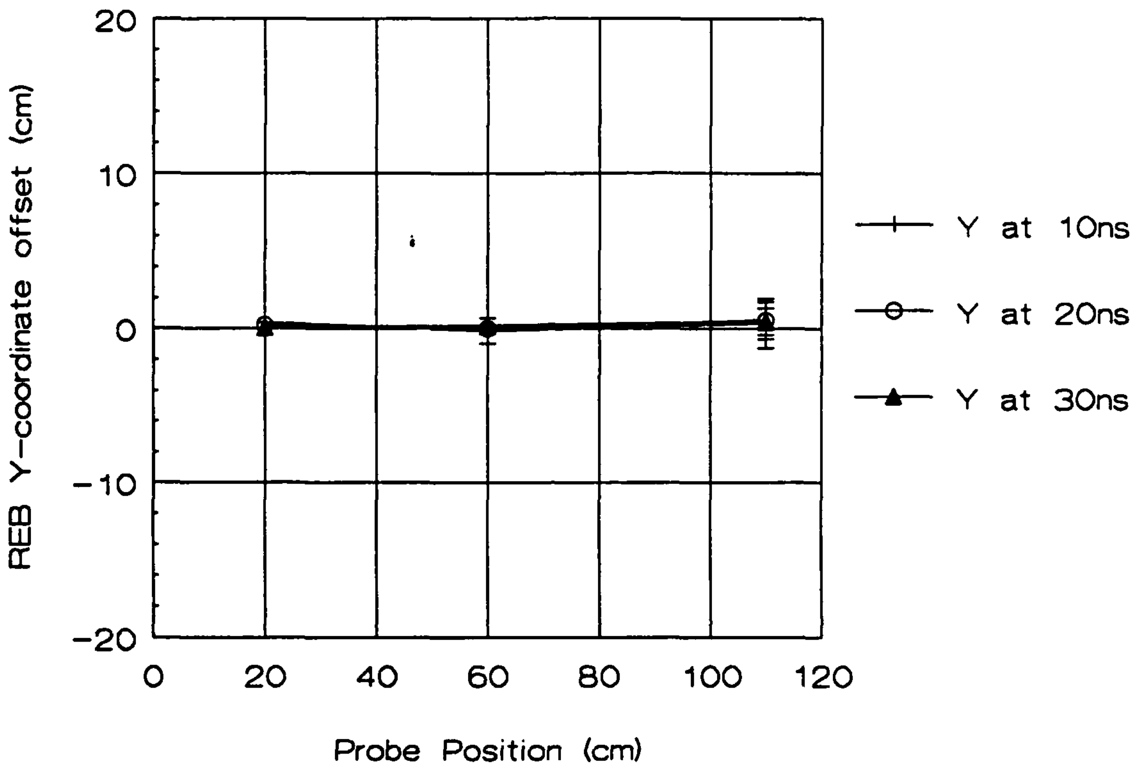

Figure 8. Beam Trajectory for the Pulserad Only, No-Channel Shots with Beam Current ≤9kA.

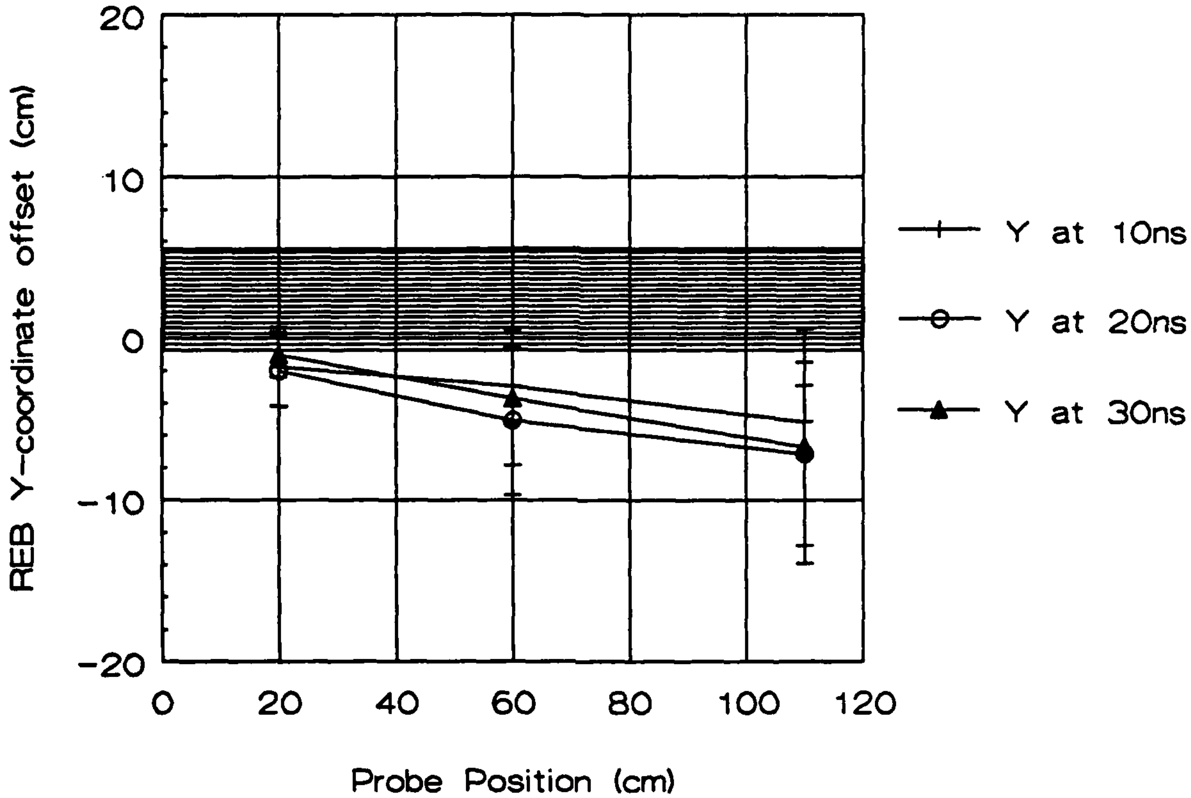

Figure 9. Beam Trajectory for the 2.6cm offset Channel Shots where the delay time between channel creation and beam injection was ≤2ms.

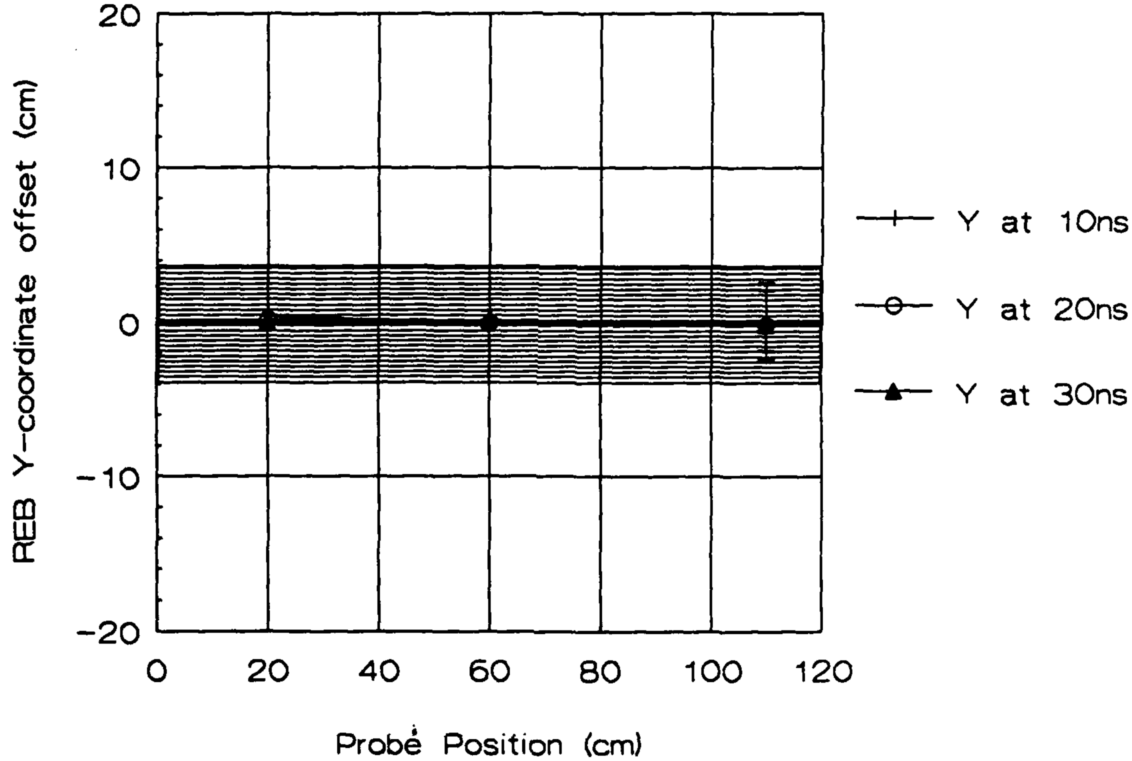

Figure 10. Beam Trajectory for the On-Axis Channel Shots with beam current ≤9kA and time delay ≥3ms.

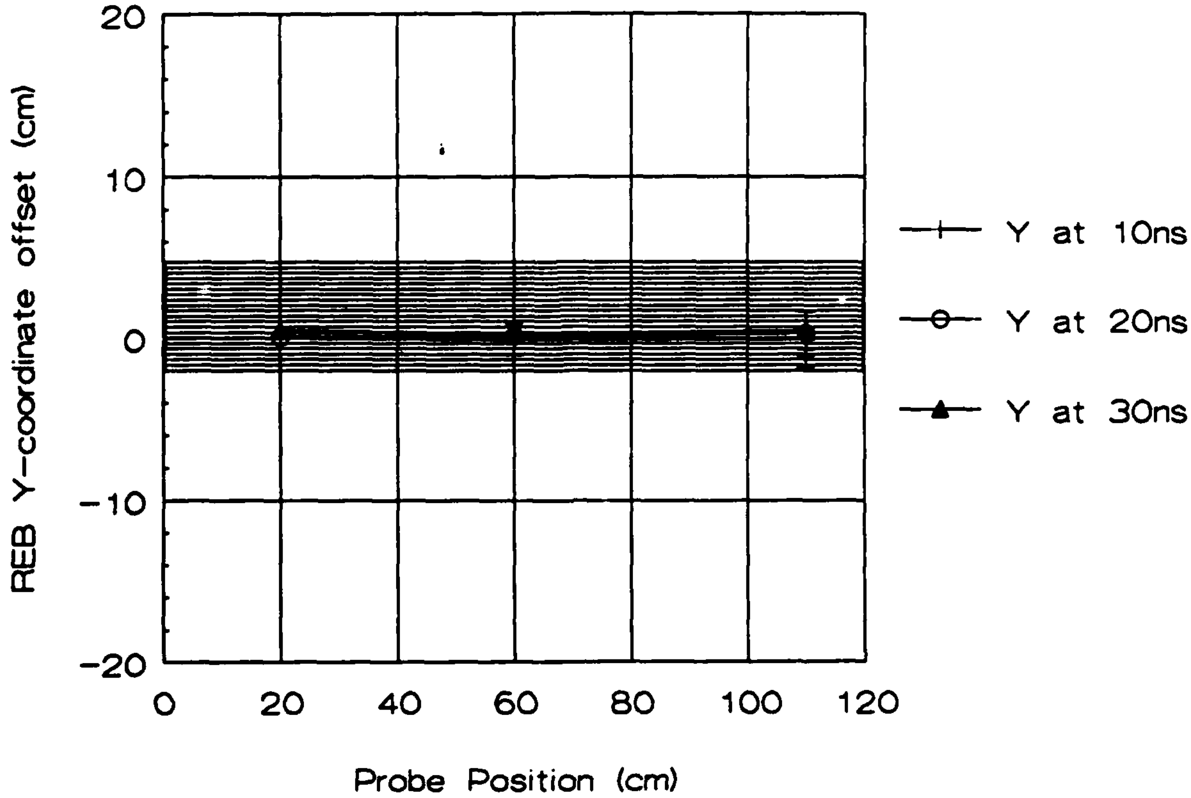

Figure 11. Beam Trajectory for the 1.4cm offset Channel Shots with the beam current ≤9kA and the delay time ≥3ms.

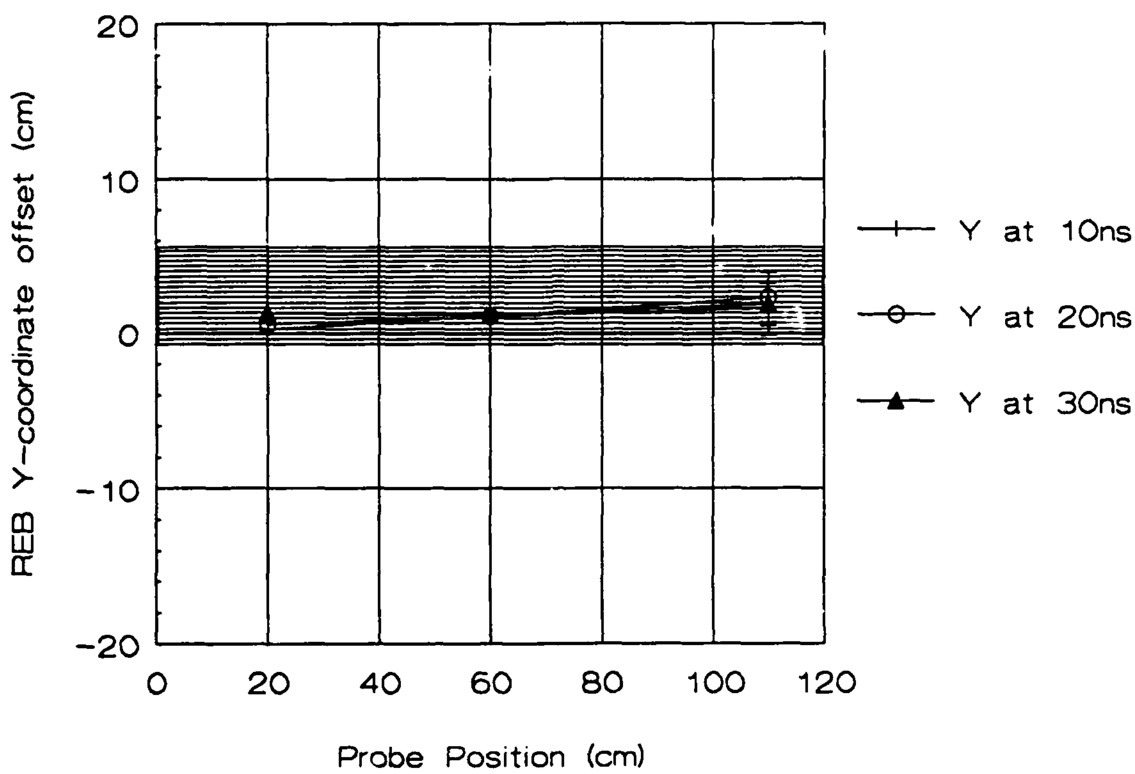

Figure 12. Beam Trajectory for the 2.6cm offset Channel Shots with the beam current ≤9kA and the delay time ≥3ms.

Distribution List*

Naval Research Laboratory
4555 Overlook Avenue, S.W.
Attn: CAPT J. J. Donegan, Jr. - Code 1000
Code 4750 (20 copies)
Dr. T. Coffey - Code 1001
Head, Office of Management & Admin - Code 1005
Deputy Head, Office of Management & Admin - Code 1005.1
Directives Staff, Office of Management & Admin - Code 1005.6
Director of Technical Services - Code 4800
ONR - Code 0124
NRL Historian - Code 2604
Dr. W. Ellis - Code 4000
Dr. J. Boris - Code 4040
Dr. M. Rosen - Code 4650
Dr. S. Ossakow - Code 4700 (26 copies)
Dr. V. Patel - Code 4701
Dr. W. Manheimer - Code 4707
Dr. A. Robson - Code 4708
Dr. J. Davis - Code 4720
Dr. S. Bodner - Code 4730
Dr. R. Meger - Code 4750
Dr. J. Antoniades - Code 4751
Dr. T. Peyser - Code 4751
Dr. D. Murphy - Code 4751 (50 copies)
Mr. M. Myers - Code 4751
Dr. R. Pechacek - Code 4750.1
Dr. G. Cooperstein - Code 4770
Dr. B. Ripin - Code 4780
Dr. A. Ali - Code 4780
Dr. M. Lampe - Code 4790
Dr. D. Colombant - Code 4790
Dr. R. Fernsler - Code 4790
Dr. I. Haber - Code 4790
Dr. R. F. Hubbard - Code 4790
Dr. G. Joyce - Code 4790
Dr. Y. Lau - Code 4790
Dr. S. P. Slinker - Code 4790
Dr. P. Sprangle - Code 4790
Dr. C. M. Tang - 4790
Dr. J. Krall - Code 4790
Dr. S. Gold - Code 4793
Dr. C. Kapetanakos - Code 4795
Library - Code 4820 (22 copies)
D. Wilbanks - Code 4834
Code 1220

Advanced Scientific Concepts, Inc.
2441 Foothill Lane
Santa Barbara, CA 93105
Attn: Dr. Roger Stettner

Advanced Technologies Research
14900 Sweitzer Lane
Laurel, MD 20707
Attn: Mr. Daniel Weldman

The Aerospace Corporation
Mail Stop M2-269
P. O. Box 92957
Los Angeles, CA 90009
Attn: Dr. David L. McKenzie
Dr. Carl J. Rice

AFATL/DLJW
Elgin Force Base, FL 32542
Attn: MAJ Louis W. Seller, Jr.

Air Force Office of Scientific Research
Physical and Geophysical Sciences
Bolling Air Force Base
Washington, DC 20332
Attn: Major Bruce Smith

Air Force Weapons Laboratory
Kirtland Air Force Base
Albuquerque, NM 87117-6008
Attn: Dr. William L. Baker (AFWL/NTYP)
Dr. Brendan B. Godfrey
Dr. Inara Kuck

Applied Physics Laboratory
The Johns Hopkins University
Asst. to Dir. for Tech. Assessment
Johns Hopkins Road
Laurel, MD 20707
Attn: Dr. Samuel Koslov

U. S. Army Ballistics Research Laboratory
Aberdeen Proving Ground, Maryland 21005
Attn: Dr. Donald Eccleshall (DRXBR-BM)
Dr. Anand Prakash
Dr. Clinton Hollandsworth

Avco Everett Research Laboratory
2385 Revere Beach Pkwy
Everett, Massachusetts 02149
Attn: Dr. R. Patrick
Dr. Dennis Reilly

Ballena Systems Corporation
P. O. Box 752
Alameda, CA 94501
Attn: Dr. Adrian C. Smith
Dr. William E. Wright

Ballistic Missile Def. Ad. Tech. Ctr.
P.O. Box 1500
Huntsville, Alabama 35807
Attn: Dr. M. Hawie (BMDSATC-1)
Dr. M. J. Lavan (BMDATC-E)
Mr. Dan Whitener

The Boeing Aerospace Company
MS-2E30
Box 3999
Seattle, WA 98124
Attn: Dr. Robert C. Milnor

Booz, Allen, and Hamilton
Crystal Square 2, Suite 1100
1725 Jefferson Davis Highway
Arlington, VA 22202-4136
Attn: Dr. Charles M. Huddleston

Central Intelligence Agency
P.O. Box 1925
Washington, DC 20013
Attn: Dr. Jose F. Pina

Chief of Naval Material
Office of Naval Technology
MAT-0712, Room 503
800 North Quincy Street
Arlington, VA 22217
Attn: Dr. Eli Zimet

Commander
Space and Naval Warfare Systems Command
National Center 1, Room 8E08
Washington, DC 20363-5100
Attn: RADM Robert L. Topping

Cornell University
369 Upson Hall
Ithaca, NY 14853
Attn: Prof. David Hammer

Defense Advanced Research Projects Agen
1400 Wilson Blvd.
Arlington, VA 22209
Attn: Dr. H. L. Buchanan
Dr. B. Hui

Defense Nuclear Agency
Washington, DC 20305
Attn: Dr. Muhammad Owais (RAAE)
Dr. Michael Frankle
Dr. R. Gullickson
Dr. J. Farber

Department of Commerce
National Inst.of Standards and Tech.
Building 245, B-102
Washington, DC 20234
Attn: Dr. Mark A. D. Wilson
Dr. Steven M. Seltzer

Department of Energy
Washington, DC 20545
Attn: Dr. Wilmot Hess (ER20:GTN,
High Energy and Nuclear Physics)
Mr. Gerald J. Peters (G-256)

Department of the Navy
Chief of Naval Operations
The Pentagon
Washington,DC 20350
Attn: CAPT T. L. Sanders (OP981N3)
LCDR John Stanovich (OP981SDI)
LCDR Donald Melick (OP981SD)
Dr. Steve Bravy (OP981SDI)
Mr. Greg Montieth

Directed Technologies, Inc.
4001 Fairfax Drive, Suite 775
Arlington, VA 22203
Attn: Mr. Ira F. Kuhn
Dr. Nancy Chesser
Dr. Arthur Lee
Ms. Marla Shain

Directed Technologies, Inc.
5945 Pacific Center Blvd.
Suite 510
San Diego, CA 92121
Attn: Dr. Robert A. Jacobsen

HQ Foreign Technology Division
Wright-Patterson AFB, OH 45433
Attn: TQTD/Mr. C. Joseph Butler

FM Technologies, Inc.
10529B Braddock Road
Fairfax, VA 22032
Attn: Dr. F. M. Mako

GA Technologies, Inc.
P. O. Box 85608
Code 02/503
San Diego, CA 93138
Attn: Dr. Vincent Chen
Dr. Hiroyuki Ikez

General Dynamics Corporation
1745 Jefferson Davis Highway
Suite 1000
Arlington, VA 22202
Attn: Dr. Daniel W. Roth

General Dynamics Corporation
Pomona Division
1675 W. Mission Blvd.
P. O. Box 2507
Pomona, CA 92769-2507
Attn: Dr. Ken W. Hawko
Mr. C. L. Featherstone

Grumman Corporation
Grumman Aerospace Research Ctr.
Bethpage, NY 11714-3580
Attn: Dr. Richard G. Madonna

Headquarters, Department of Army
DAMOFDE, Room 2D547
The Pentagon
Washington, DC 20310-0460
Attn: LTCOL Lou Goldberg

HQ Foreign Technology Division
Wright-Patterson AFB, OH 45433
Attn: TUTD/Dr. C. Joseph Butler

HQ USAF/TXN
Patrick Air Force Base, FL 32925
Attn: CAPT Joseph Nicholas

Hudson Institute
Center for Naval Analyses
Alexandria, VA 22302
Attn: Dr. F. Bomse

Hy-Tech Research Corp.
P. O. Box 3422 FSS
Radford, VA 24143
Attn: Dr. Edward Yadlowsky

Idaho Engineering National Lab.
P. O. Box 1625
Idaho Falls, ID 83415
Attn: Dr. Francis Tsang

Institute for Defense Analyses
1801 N. Beauregard Street
Alexandria, VA 22311
Attn: Dr. Deborah Levin
Ms. M. Smith

IRT Corporation
3030 Callan Road
San Diego, CA 92121
Attn: Dr. David Phelps

JAYCOR
39650 Libery Street, Suite 320
Freemont, CA 94538
Attn: Dr. Kendal Casey

Joint Institute for Laboratory Astrophysics
National Bureau of Standards and University of Colorado
Boulder, CO 80309
Attn: Dr. Arthur V. Phelps

Kaman Sciences
P. O. Drawer QQ
Santa Barbara, CA 93102
Attn: Dr. W. Hobbs

La Jolla Institute
P. O. Box 1434
La Jolla, CA 92038
Attn: Dr. K. Brueckner

Lawrence Berkeley Laboratory
University of California
Berkeley, CA 94720
Attn: Dr. Edward P. Lee
Dr. Thomas Fessenden
Dr. William Fawley
Dr. Roger Bangerter

Lawrence Livermore National Laboratory
University of California
Livermore, California 94550
Attn: Dr. Ed Farley
Dr. George Kamin
Dr. V. Kelvin Neil
Dr. Arthur C. Paul
Mr. Louis Reginato
Dr. Simon S. Yu
Dr. Frank Chambers
Dr. James W.-K. Mark, L-477
Dr. William Barletta
Dr. William Sharp
Dr. John Clark
Dr. George J. Caporaso
Dr. Donald Prosnitz
Dr. Y. P. Chong
Dr. Hans Kruger
Dr. Thaddeus J. Orzechowski
Dr. John T. Weir

Lockheed Missiles and Space Co.
3251 Hanover St.
Bldg. 205, Dept 92-20
Palo Alto, CA 94304
Attn: Dr. John Siambis

Los Alamos National Laboratory
P.O. Box 1663
Los Alamos, NM 87545
Attn: Dr. L. Thode
Mr. R. Carlson, MS-P940
Dr. Carl Ekdahl, MS-D410
Dr. Joseph Mack
Dr. Daniel S. Prono
Dr. S. Czuchlewski

Maxwell Laboratories Inc.
8888 Balboa Avenue
San Diego, CA 92123
Attn: Dr. Ken Whitham
Dr. S. Echouse

McDonnell Douglas Research Laboratories
Dept. 223, Bldg. 33, Level 45
Box 516
St. Louis, MO 63166
Attn: Dr. Carl Leader

Mission Research Corporation
1720 Randolph Road, S.E.
Albuquerque, NM 87106
Attn: Dr. Thomas Hughes
Dr. Lawrence Wright
Dr. Kenneth Struve
Dr. Michael Mostrom
Dr. Dale Welch

Mission Research Corporation
P. O. Drawer 719
Santa Barbara, California 93102
Attn: Dr. C. Longmire
Dr. N. Carron

Mission Research Corporation
8560 Cinderbed Road
Suite 700
Newington, VA 22122
Attn: Dr. Khanh Nguyen

National Inst. of Standards & Tech.
Gaithersburg, Maryland 20760
Attn: Dr. Mark Wilson

National Inst. of Standards & Tech.
Radiation Physics Bldg. Room C229
Washington, DC 20234
Attn: Dr. Wayne Cassatt

National Security Agency
4928 College Avenue
College Park, MD 20740
Attn: Dr. Albert J. Leyendecker

Naval Ocean Systems Center
San Diego, CA 92152
Attn: CAPT James Fontana

Naval Postgraduate School
Physics Department (Code 61)
Monterey, CA 93940
Attn: Prof. John R. Neighbours
Prof. Fred Buskirk

Naval Surface Warfare Center
Dahlgren, VA 22448-5000
Attn: Mr. Lawrence Luessen
Dr. S. L. Moran

Naval Surface Warfare Center
White Oak Laboratory
Code R-41
Silver Spring, Maryland 20903-5000
Attn: CAPT R. P. Fuscaldo
CAPT R. W. Moore
Mr. Carl Larson
Dr. Robert DeWitt
Dr. Ralph Schneider
Dr. Joel Miller
Dr. Stanley Stern
Dr. H. S. Uhm
Dr. R. Fiorito
Dr. R. Stark
Dr. H. C. Chen
Mrs. Carolyn Fisher (G42)
Dr. Eugene E. Nolting (H23)

Naval Technical Intelligence Center
Code DA52
4301 Suitland Road
Washington, DC 20395
Attn: Mr. Mark Chapman

Office of the Chief of Naval Operations
Strategic and Theatre Nuclear Warfare D
OP-654E4
The Pentagon
Washington, DC 20350
Attn: Dr. Yong S. Park

Office of Naval Research
800 North Quincy Street
Arlington, VA 22217
Attn: Dr. C. W. Roberson
Dr. F. Saalfeld

Office of Naval Research (2 copies)
Department of the Navy
Code 01231C
Arlington, VA 22217

Office of Under Secretary of Defense
Research and Engineering
Room 3E1034
The Pentagon
Washington, DC 20301
Attn: Dr. John MacCallum

OSWR
P. O. Box 1925
Washington, DC 20013
Attn: Dr. Jose F. Pina

PhotoMetrics, Inc.
4 Arrow Drive
Woburn, MA 01801
Attn: Dr. Irving Kofsky

Physics International, Inc.
2700 Merced Street
San Leandro, CA. 94577
Attn: Dr. E. Goldman
Dr. James Benford
Dr. George B. Frazier
Mr. Ralph Genuario

Princeton University
Plasma Physics Laboratory
Princeton, NJ 08540
Attn: Dr. Francis Perkins, Jr.

Pulse Sciences, Inc.
600 McCormack Street
San Leandro, CA 94577
Attn: Dr. Sidney Putnam
Dr. Vernon Bailey

Pulse Sciences, Inc.
2001 Wilshire Boulevard
Suite 600
Santa Monica, CA 90403
Attn: Dr. John R. Bayless

R&D Associates
301A South West Street
Alexandria, VA 22314
Attn: Mr. Ihor Vitkovitsky

The Rand Corporation
2100 M Street, NW
Washington, DC 20037
Attn: Dr. Nikita Wells
Mr. Simon Kassel

Sandia National Laboratory
Albuquerque, NM 87115
Attn: Dr. Collins Clark
Dr. Charles Frost
Dr. Michael G. Mazarakis/1272
Dr. John Wagner/1241
Dr. Ron Lipinski/1274
Dr. James Poukey
Dr. Milton J. Clauser/1261
Dr. Kenneth R. Prestwich/1240
Dr. Kevin O'Brien
Dr. Isaac R. Shokair
Dr. J. Pace VanDevender/1200
Dr. J. T. Crow
Dr. S. Shope
Dr. B. N. Turman
Dr. C. Olson
Dr. Malcolm Buttram
Mr. Charles Crist
Dr. Susan Fisher
Dr. Gordon T. Leifeste
Dr. Raymond W. Lemke
Dr. Juan Ramirez
Dr. James Rice

Science Applications Intl. Corp.
2109 Air Park Road, S. E.
Albuquerque, NM 87106
Attn: Dr. R. Richardson
Dr. Michael D. Haworth
Dr. Alan J. Toepfer

Science Applications Intl. Corp.
5150 El Camino Road
Los Altos, CA 94022
Attn: Dr. R. R. Johnston
Dr. Leon Feinstein
Dr. Douglas Keeley

Science Applications Intl. Corp.
1710 Goodridge Drive
McLean, VA 22102
Attn: Mr. W. Chadsey
Dr. A Drobot
Dr. K. Papadopoulos
Dr. William W. Rienstra
Dr. Alfred Mondelli
Dr. D. Chernin
Dr. R. Tsang
Dr. J. Petillo

Science Research Laboratory, Inc.
1600 Wilson Boulevard
Suite 1200
Arlington, VA 22209
Attn: Dr. Joseph Mangano
Dr. Daniel Birx

Commander
Space & Naval Warfare Systems Command
PMW-145
Washington, DC 20363-5100
Attn: Mr. D. Merritt

Space Power Institute
315 Leach Science Center
Auburn University
Auburn, AL 36845=3501
Attn: Prof. M. Frank Rose

Spectra Technology
2755 Northup Way
Bellevue, WA 98004
Attn: Dr. Dennis Lowenthal

SRI International
PSO-15
Molecular Physics Laboratory
333 Ravenswood Avenue
Menlo Park, CA 94025
Attn: Dr. Donald Eckstrom
Dr. Kenneth R. Stalder

Strategic Defense Initiative Org.
SDIO/T/DEO
The Pentagon
Washington, DC 20301-7100
Attn: COL Thomas Meyer (DEWO)
LTC Michael toole (DEWO)
MAJ J. Wills
Dr. Dwight Duston
LTC Ed Pogue
Dr. Kevin Probst
Dr. Charles Sharn

System Planning Corporation
1500 Wilson Boulevard, Room 1213W
Arlington, VA 22209
Attn: Mr. James T. Lacatski

Titan/Spectron, Inc.
P. O. Box 4399
Albuquerque, NM 87196
Attn: Dr. R. Bruce Miller
Dr. John Smith

Titan Systems, Inc.
5910 Pacific Center Blvd.
San Diego, CA 92121
Attn: Dr. R. M. Dowe, Jr.

Tetra Corporation
4905 Hawkins Street, N. E.
Albuquerque, NM 87109-4345
Attn: Mr. William Money

University of California
Physics Department
Irvine, CA 92664
Attn: Dr. Gregory Benford
Dr. Norman Rostoker

University of California
San Diego, CA 92110
Attn: Dr. Marshall N. Rosenbluth

UCLA
Physics Department
Los Angeles, CA 90024
Attn: Dr. F. Chen
Dr. J. Dawson
Dr. W. Barletta

University of Colorado
Dept. of Astrophysical, Planetary & Atmospheric Sciences
Boulder, CO 80309
Attn: Dr. Scott Robertson

University of Illinois at Chicago
Dept. of Physics
P. O. Box 4348
Chicago, IL 60680
Attn: Dr. Charles K. Rhodes

University of Maryland
College Park, MD 20742
Attn: Dr. J. Goldhar
Dr. W. Destler
Dr. C. Striffler
Dr.Moon-Jhong Rhee
Dr. Dr. Reiser

University of Michigan
Dept. of Nuclear Engineering
Ann Arbor, MI 48109
Attn: Prof. Terry Kammash
Prof. R. Gilgenbach

University of New Mexico
Dept. of Chem. & Nuclear Engineering
Albuquerque, NM 87131
Attn: Prof. Stanley Humphries

Commander
U. S. Army Laboratory Command
2800 Powder Mill Road
Adelphi, MD 20783-1145
Attn: George Albrecht (AMSLC-TP-PL)

U. S. Army Combined Army Center
ATZL-CAG
Ft. Leavenworth, KS 68027-5000
Attn: LTC Orville Stokes

Yale University
Mason Laboratory
New Haven, CN 06520
Attn: Dr. Ira Bernstein

Director of Research
U.S. Naval Academy
Annapolis, MD 21402 (2 copies)

Timothy Calderwood
Naval Research Laboratory
Code 4830